Electrochemical characterization of temperature dependence of a Lithium-ion battery

O. B. Saban[1,*], E. Güzel[2], M. F. Serincan[1], M. A. Arslan[1]

[1]Department of Mechanical Engineering, Gebze Technical University, Kocaeli, Turkey

[2]Department of Electronics Engineering, Gebze Technical University, Kocaeli, Turkey

ABSTRACT

Lithium-ion batteries are one of the most preferred energy storage devices for today's world due to their high capacity and power density. 18650-type cylindrical Lithium-ion batteries are commonly used in different application areas such as automotive and space industry for their stability, sustainability, and applicability. Thus, to investigate the battery's performance and develop its technology, analysing the electrochemical reactions that occurred inside the battery is crucial. Discharge tests, pulse tests, and Electrochemical Impedance Spectroscopy (EIS) are frequently used methods to understand the electrochemical performance of the batteries. The EIS measurements of fully charged batteries are conducted between 10 mHz and 200 kHz for a deep understanding of polarization processes. In this study, the electrochemical stabilities of cylindrical Sony Murata 18650-type Lithium-ion batteries in different ambient temperatures at various states of charge are analysed with two types of equivalent circuit modelling methods.

Cite this article: O. B. Saban, E. Güzel, M. F. Serincan, M. A. Arslan, "Electrochemical characterization of temperature dependence of a Lithium-ion battery" *Turkish Journal of Electromechanics & Energy*, 6(1), pp.31-38, 2021.

1. INTRODUCTION

Due to the favorable energy rate, power, and stability of batteries, automotive, defence, space industries, technology companies mostly use these electrochemical energy storage systems in different areas. Batteries can be arranged into various classifications by considering the chemical composition, size, and use cases. Yet, there are two principal types of batteries: primary batteries and secondary batteries [1]. While primary batteries are not rechargeable, secondary batteries can switch chemical responses to electrical power many times. Also, secondary batteries can be arranged in several different types such as Nickel Cadmium (Ni-Cd), Nickel-Metal Hydride (Ni-MH), Lead Acid, and Lithium-ion (Li-ion) due to their chemical decompositions. The characteristics of widely used batteries, such as voltage values, operating temperature range, are listed in Table 1 [2]. According to the studies, it is possible to reach 2000 cycles depending on the chemical structure, manufacturing processes, design criteria, and operating conditions of the cells' rechargeable Li-ion batteries.

Table 1. Properties of widely used batteries.

Battery Type	Nominal Voltage (V)	Energy Density (Wh/kg)	Life Cycle	Min. Operating Temp. (°C)	Max. Operating Temp. (°C)
Lead Acid	2.0	35	1000	-15	50
Nickel-Cadmium	1.2	50-80	2000	-20	50
Lithium-Ion	3.6	118-250	2000	-20	60
Lithium-Ion Polymer	3.7	130-225	1200	-20	60
Lithium-Iron Phosphate	3.2	120	2000	-45	70
Lithium-Air	2.9	1300-2000	100	-10	70

Among the most significant parameters, the life cycle and capacity of Li-ion batteries are affected by operating conditions such as ambient temperature, current flow, and charge state. Although the operating temperature range of Li-ion batteries from -20°C to 60°C, most of the commercial Li-ion batteries work under an optimal temperature range of 15 – 35°C. According to Waldmann *et al.*, low and high operating temperature values dramatically affect the battery's life [3]. While below 25°C,
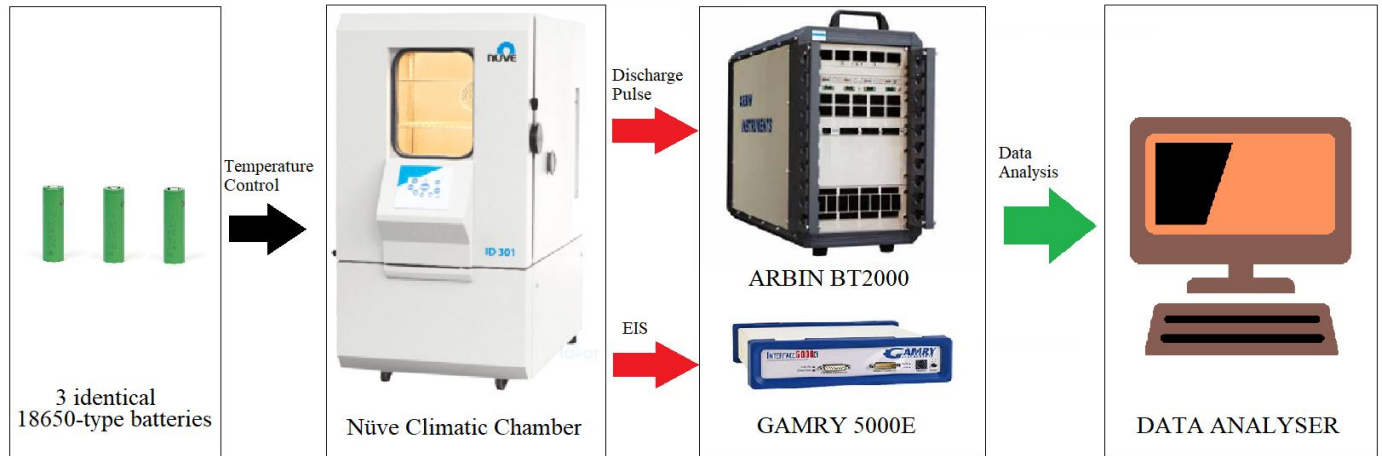
Fig. 1. Experimental setup.

significant degradation occurs due to the Lithium plating on the negative electrode, above 25°C, both solid-electrolyte interface (SEI) thickening and degradation in positive and negative electrodes [4, 5]. Flowing current through the battery has also a significant impact on the battery's life. The high current flow rate in charge and discharge processes causes the temperature to rise, damaged electrode structure due to the rapid reactions, lithium deposition [6–8]. Further, the battery's state of charge (SOC) can be determined by the application's needs. Usually, higher SOC leads to side reactions such as SEI thickening and electrode decomposition [9, 10]. On the other hand, lower SOC may lead to the current collectors corrosion and disordered active material structure [11]. Therefore, investigating the effects of operating conditions may help to predict the electrochemical stability window of Li-ion batteries.

This study examines the impact of operating temperature on commercial Li-ion batteries by discharge tests, pulse tests, and electrochemical impedance measurements. Discharge tests are one of the most used measurement methods that provide a relation between voltage change and capacity and internal resistance by applying continuous current to the system. On the other hand, pulse tests are a widely used method for parameterizing resistive and capacitive behavior in the time domain and SOC estimation by applying currents with relaxations. Another powerful method to predict the dynamic behavior of batteries is electrochemical impedance spectroscopy (EIS), which represents the voltage (or current) response of the perturbed system in the frequency domain. The resultant perturbation-answer ratio is called impedance. It is a complex variable with real and imaginary parts that provide information about the system's capacitive, resistive, and inductive behavior. Nyquist diagram, one of the commonly used impedance representation methods, allows analyzing battery kinetics by evaluating semi-circles and diffusion tail. In this study, to identify the electrical characteristics with electrical circuit elements of the batteries from the measurement data, equivalent circuit modelling (ECM) is used.

2. EXPERIMENTAL

The experimental part of this study consists of three processes under various ambient temperatures (0°C, 25°C and 40°C), discharge tests, pulse tests and EIS measurements. Three identical commercial Sony US18650VTC5 Cylindrical 2.5 Ah 18650-type cylindrical lithium-ion batteries are used for the experiments to project the temperature dependence of electrochemical characteristics. The cells are made from Lithium Nickel Manganese Cobalt Oxide (NMC) material as the positive electrode, which provides high power, high energy density and high cycle life, graphite material as the negative electrode and LP-30 electrolyte. Battery tests are performed in Nüve Climatic Chambers to set and control the desired ambient temperature. Gamry 5000E is used for EIS measurements, ARBIN BT2000 Battery Tester devices are used for obtaining and monitoring the discharge tests and pulse tests. Experimental setup is shown in Figure 1.

Considering the battery properties shown in Table 2 [12], discharge measurements are performed constant current – constant voltage technique. Batteries are charged until 4.2 V with constant current (2.5 A) and constant voltage (4.2 V) until the current drops below 100 mA, and the discharge process is performed under constant current (2.5 A) until the cut-off voltage (2.5 V) limit in desired ambient temperatures. Besides, various discharge current flows (0.5 A, 1.25 A and 2.5 A) are applied to the batteries in different operating temperatures by constant current – constant voltage technique.

Pulse tests are carried out using the ARBIN BT2000 Battery Tester with the desired pulse current discharge rate and Nüve Climate Chamber to control the ambient temperature. These tests are repeated at three different temperatures to fully charged batteries with the application of 20 pulses with 90 minutes relaxation times until the cut-off voltage limit with 2.5 A discharge current. As for calculating the resistance and capacitance values, an equivalent circuit model developed by MATLAB is used.

EIS measurements are performed with the frequency range between $10\,mHz - 200\,kHz$ and five mV/s scanning rate in different SOCs of the batteries at each operating temperature. Since the SOC of the battery isn't related to open circuit potential directly, discharge tests and pulse tests are used for SOC determination. Simply, the SOC of the batteries can be estimated as the ratio of the amount of capacity at a time $Q(t)$ and the amount of maximum capacity Q_{max}.

$$SOC(t) = \frac{Q(t)}{Q_{max}} \qquad (1)$$

Table 2. Properties of Sony US18650VTC5 18650 type cylindrical lithium-ion battery.

Property	Unit	Value
Diameter	mm	18.35
Length	mm	65.2
Weight	g	44.3
Nominal Voltage	V	3.6
Charge-up Voltage	V	4.2
Discharge cut-off Voltage	V	2.5
Internal Impedance at AC-1 kHz	mΩ	13.0
Nominal Capacity (0.2 C discharge at 25°C)	mAh	2577

3. RESULTS

As discussed earlier, the electrochemical performance and capacity of the batteries are highly dependent on the ambient temperature. Many studies show that low diffusivity and conductivity in the electrolyte and the slow-moving charge transfer kinetics and solid-state diffusion in the anode and cathode materials occur in low ambient temperature [13]. Also, fast reactions may damage the electrodes and the electrolyte solution. All these side reactions result in decreased available capacity and power density. To conclude the temperature effect, as the first step, the discharge characteristics of the batteries should be analysed. As shown in Figure 2(a), 2.5 A discharge current is applied to fresh batteries in different ambient temperatures. At 0°C, while discharge capacity is around 2086 mAh, approximately 20% lower than the discharge capacity at 25°C and 40°C. On the other hand, at 40°C, available capacity is relatively higher (3%) than capacity at 25°C. Although high-temperature-operated batteries' long-term performance is low, short-term discharge performance is quite well due to faster reactions and fast diffusion kinetics [14]. Figure 2(b-d) represent the current flow dependence of the studied batteries in different operation temperatures. As the lower current rates are applied, it is possible to reach higher discharge capacities. Moreover, at 0°C, rapid voltage drops (activation loss) can be eliminated by lowering the discharge current.
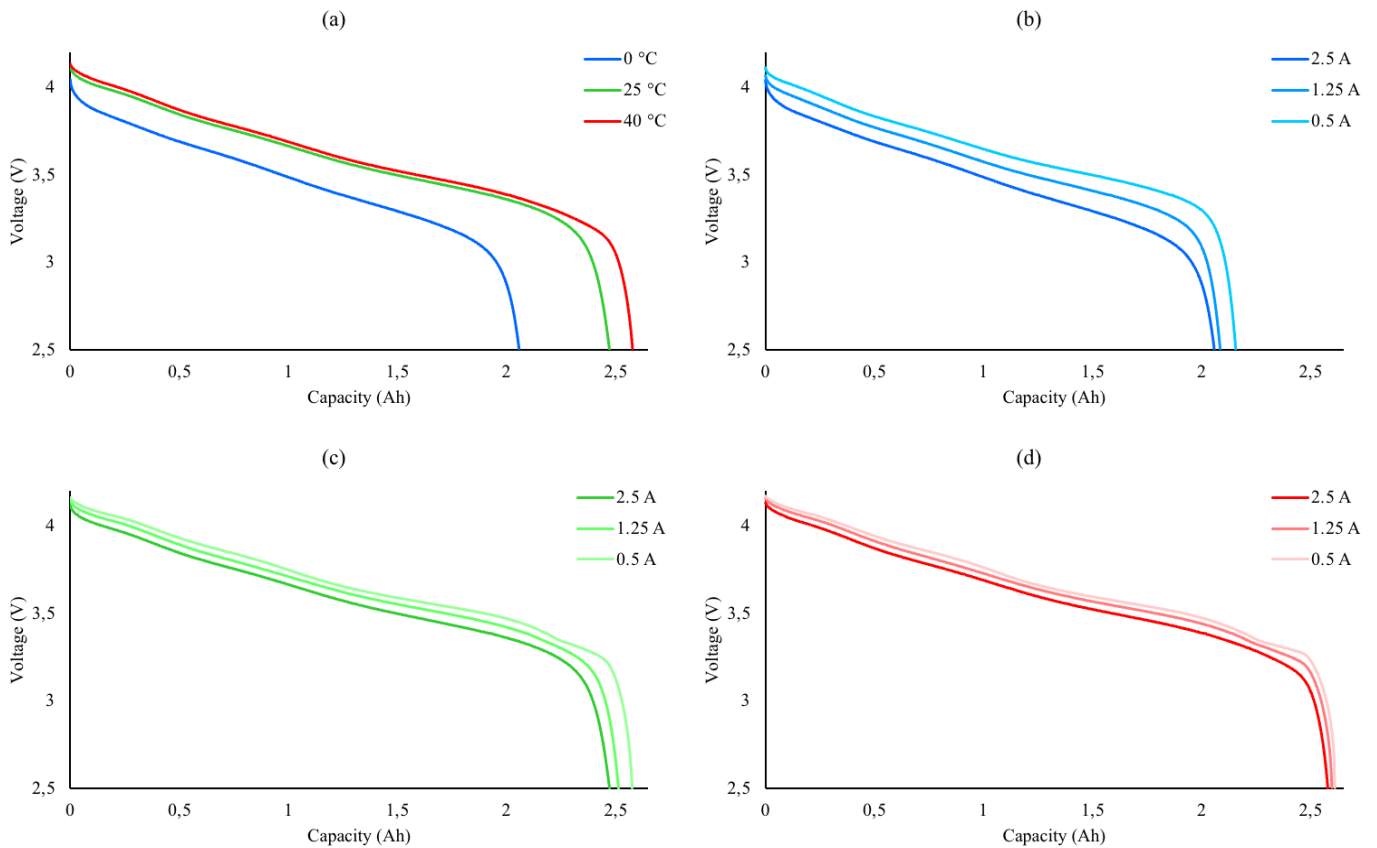

Fig. 2. Temperature dependence of discharge process of the battery. (a) 2.5 A discharge current at different ambient temperatures. (b), (c) and (d) represent various discharge currents at 0°C, 25°C and, 40°C, respectively.

As for calculating SOC values, the ratio between the capacity value and maximum capacity is used. Table 3 represents the SOC values with 20% decrements from 100% to 0%. As the maximum capacity equals to maximum discharge capacity, the current capacity can be evaluated as:

$$Q(t) = Q_{max} - Q_{disch} \tag{2}$$

Table 3. SOC, i.e. discharge capacity and voltage values of experimental cells at different ambient temperatures.

SOC (%)	0 °C		25 °C		40 °C	
	Discharge Capacity (mAh)	Voltage (V)	Discharge Capacity (mAh)	Voltage (V)	Discharge Capacity (mAh)	Voltage (V)
100	0	4.07	0	4.14	0	4.16
80	417.21	3.81	502.90	3.89	519.45	3.90
60	834.01	3.64	1005.48	3.71	1038.69	3.71
40	1251.23	3.49	1508.99	3.55	1558.23	3.56
20	1668.07	3.35	2011.15	3.42	2077.73	3.41
0	2085.61	2.50	2514.34	2.50	2597.10	2.51

As shown in Figure 3, pulse tests are obtained at different ambient temperatures. Due to the low-temperature behaviour of electrochemical reactions, at 0°C, voltage gains of pulses responded higher concerning the discharge trend of the battery. Additionally, as the heat is generated during each pulse, conductivities of the electrodes and diffusion kinetics of the electrolyte solution increase, which lead to voltage gains at relaxation periods.
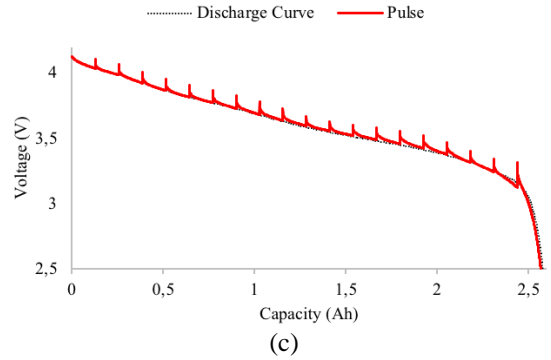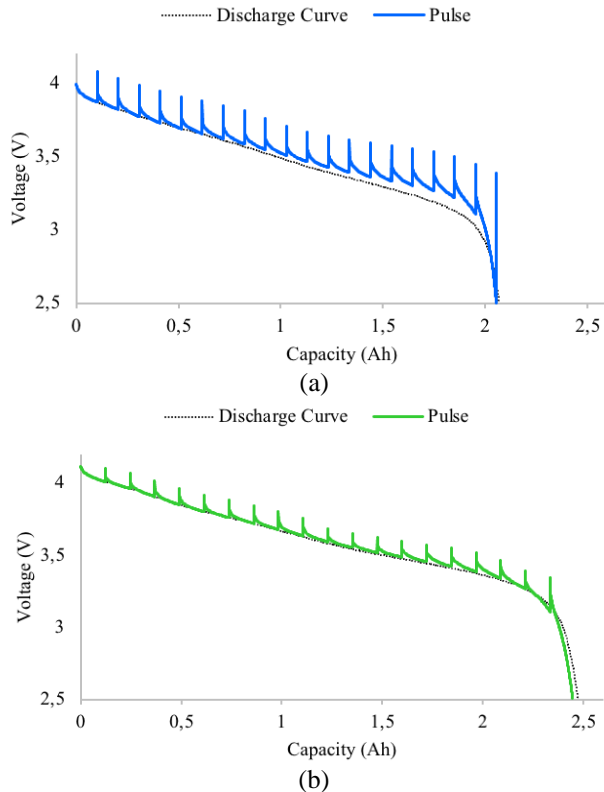

(a)

(b)

(c)

Fig. 3. Pulse characteristics of the batteries under (a) 0 °C, (b) 25 °C, (c) 40 °C ambient temperatures.

Pulse tests are the widely used method to predict DC electrochemical characteristics of the batteries in various loading conditions. ECM is a beneficial method to identify resistive and capacitive behavior as well as diffusion characteristics of an electrochemical system by using passive elements such as capacitor (C), resistance (R), and inductance (L). On the other hand, as the electrochemical systems are not ideal circuits, constant phase element (CPE) to model the impurities like porosity can be used.

In the pulse examination part, the DC resistance and capacitance values (obtained from pulse tests) of the batteries in different temperatures, considering Lithium-ion mass transfer phenomena [15], 1 RC ECM, which is parallel connected charge transfer resistance and charge transfer capacitance connected series with internal resistance is used, as seen in Figure 4. As the potential of the cell V depends on applied current, I and resistance and capacitance values of the batteries, the circuit equation of the cells can be derived by using Kirchhoff's Law. While R_i indicates the resistive losses, R_{CT} represents the equivalent polarization resistance, and C_{CT} denotes equivalent polarization resistance due to charge transfer. Figure 5 shows the results obtained from pulse tests.

$$\frac{dV_c}{dt} = -\frac{1}{R_{CT}C_{CT}} \times V_c(t) + \frac{1}{C_{CT}} \times i(t) \tag{3}$$

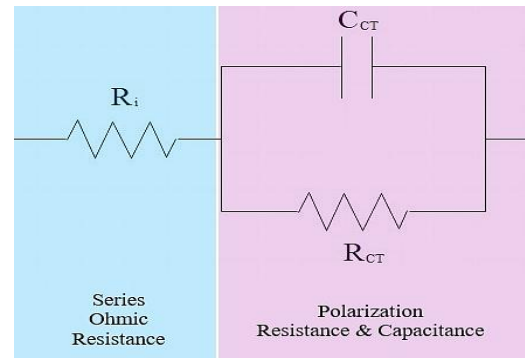$$V(t) = V_{ocp}(t) - V_c(t) - R_i \times i(t) \tag{4}$$

Fig. 4. Equivalent circuit modelling for the calculation of the R and C parameters obtained from pulse tests data.

R_{CT} and C_{CT} parameters can be calculated by considering the charge transfer processes between the electrodes and electrolyte solution using the time constant τ.
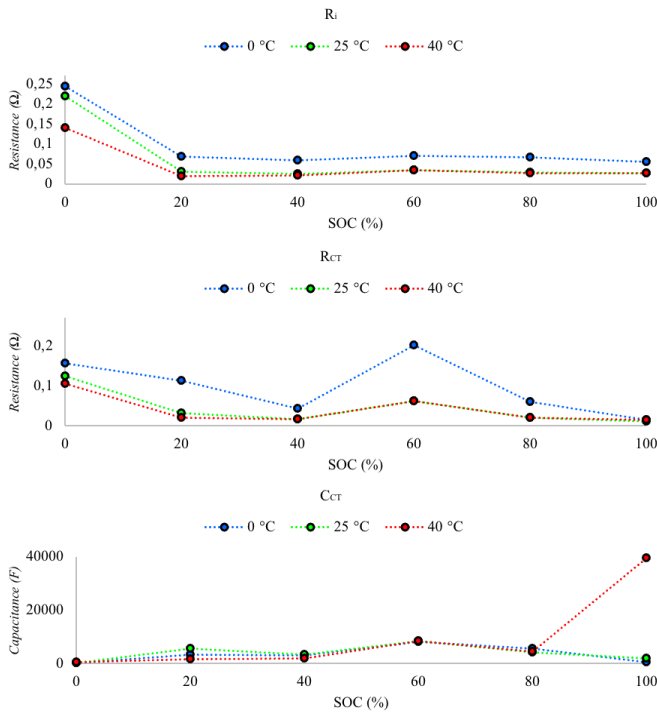
$$\tau = R_{CT} \times C_{CT} \tag{5}$$

Fig. 5. R and C parameters of the batteries at different ambient temperatures obtained from pulse tests.

R_i values obtained from pulse tests are higher than EIS results because of the different accuracy of the experimental equipment. Moreover, at 0% SOC, R_i values tend to be higher at each ambient temperature. R_I values correspond to the serial connection of charge transfer resistance and solid electrolyte interface resistance. As seen in Figure 5, while the resistance and capacitance values show a pick at all ambient temperatures at 60% SOC as expected, but at 40°C, slightly high capacitive behaviour seen at 100% SOC.

As shown in Figure 6, impedance behaviour of the battery is modelled with ECM consisting two elements: CPE and R. In the model, R_i indicates ohmic resistance. It is related to an electrolyte, separator, current collector, and electric conductivity of current collectors. At the same time, R_{SEI} and CPE_{SEI} represent the first semi-circle in the mid-high frequency region of the Nyquist diagram as the resistance of the solid electrolyte interface layer and the decomposition of organic electrolyte compounds on the surface of the graphite electrode, respectively. R_{CT} and CPE_{CT} correspond to the second semi-circle in the mid-low frequency region of the Nyquist diagram, which indicate the charge transfer impedance of the positive electrode. Lastly, CPE_{diff} is assigned with Li$^+$ diffusion in the solid phase, most likely observed in the low-frequency region in impedance spectra. Generally, the solid-state mass diffusion process is modelled with the Warburg

element, which can be considered CPE with a 45° angle ($\alpha = 0.5$) [16]. Since the batteries have impurities, the diffusion tail is modelled with CPE to obtain better fitting results.
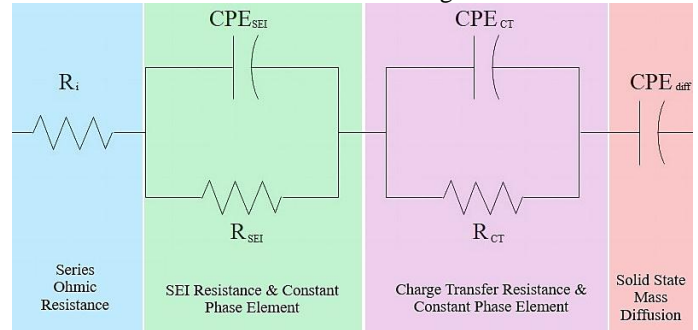

Fig. 6. Equivalent circuit model for fitting the experimental impedance data of the cells.

Figure 7 and Figure 8 show the Nyquist plots of the EIS results in different SOC values at different ambient temperatures. As shown in the figure, temperature change affects the overall impedance. The first semi-circle related to SEI formation in the graphite electrode is growing as the temperature decreases. Further, the second semi-circle, which is related to charge transfer kinetics of NMC material and diffusion tail in the low-frequency region, are also dependent on the temperature changes.
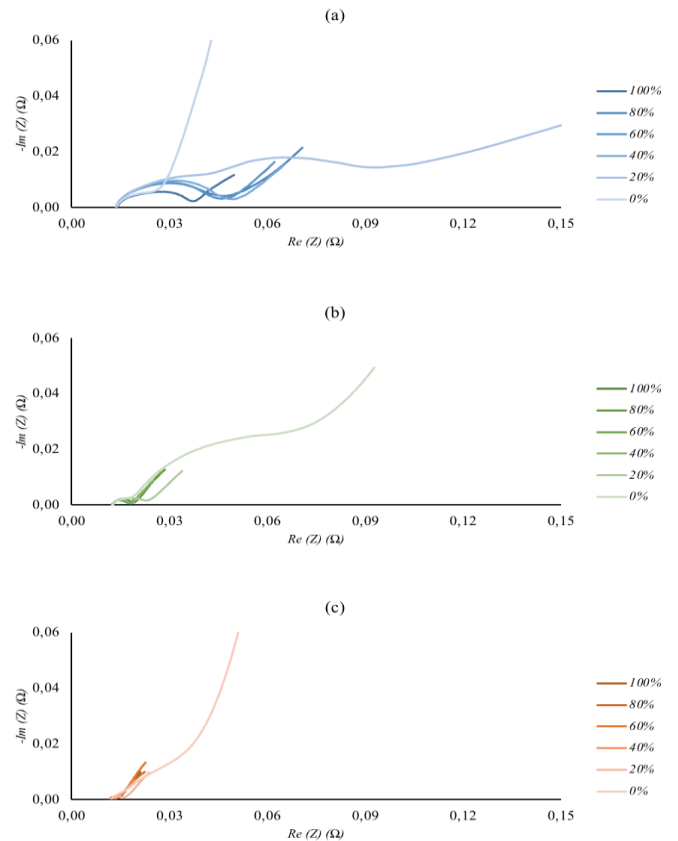

Fig. 7. (a), (b) and (c) represent the Nyquist plots of the EIS results of the battery at different SOC values at 0°C, 25°C and, 40°C, respectively.

As detailed in Figure 8 and Figure 9 , in the high-frequency region of the Nyquist diagram, R_i, which is the first intersection point with the $Re(Z)$ axis, is not changing within the change in SOC but increases while the temperature is decreasing. Besides, the change in SOC does not affect the value of the R_{SEI} element noticeably until SOC is 0%; however, the CPE_{SEI} element has the highest values when the battery is fully charged in different ambient temperatures during the experiment. The low temperature operated Li-ion batteries suffer from low cyclic life and fast capacity degradation during operation due to the volume changes in graphite electrodes and the local voltage differences, resulting in lithium deposition [17]. Therefore, the solid electrolyte interface formation is most likely to be stable in different ambient temperatures. Still, it is understandable that electrolyte channels are blocked at low temperatures since the SEI film layer got thicker. As a result of thickened SEI, lithium ions in the electrolyte can't intercalate the graphite electrode, which leads to an increase in R_i value. The second semi-circle, which corresponds to R_{CT} and CPE_{CT} elements, are observed after 20% SOC. The results show that the charge transfers impedance increases while the battery's capacity is at a lower state. On the other hand, the resistance of Li$^+$ insertion into the electrode became higher at low temperatures because the SEI film layer has thickened. CPE_{diff}, the capacitive behaviour of solid-state diffusion is after 40% SOC is slightly decreasing.

As for the comparison of the R and C parameters obtained from the pulse tests and impedance data, the relationship between

the capacitance and constant phase element can be represented with Brug's formula [18].

$$C_{CPE} = \left[CPE_n \cdot \left(\frac{1}{R_n} \right)^{\alpha-1} \right]^{\frac{1}{\alpha}} \tag{6}$$

In Equation (6), C_{CPE} indicates the capacitance calculated from the constant phase element, CPE_n and R_n denote the CPE and resistance values of the corresponding semi-circle, and α is the exponent in the equation for the CPE. When $\alpha = 1$, CPE represents a pure capacitance. On the other hand, surface heterogeneities can be modelled when $\alpha < 1$ [19]. The resultant electrochemical analysis for α and capacitance values at each operation temperature are shown in Table 4.

Table 4. Capacitance values of the first semi-circle.

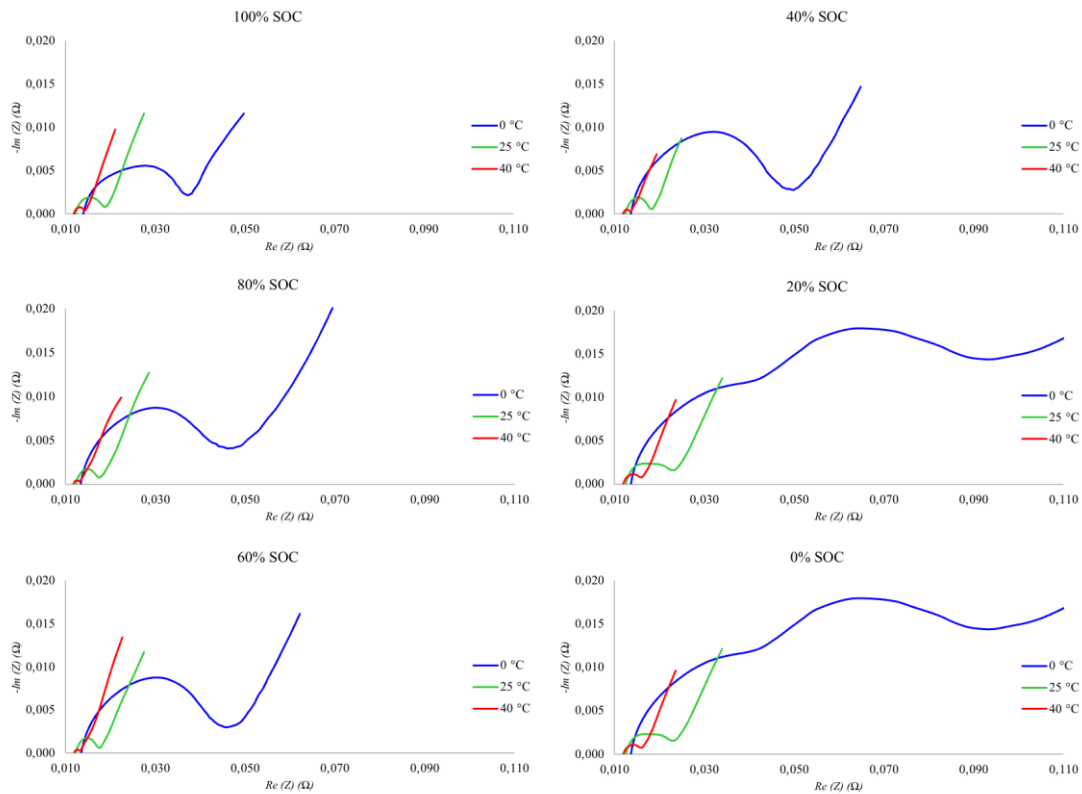| SOC | Operation Temperature | | | | | |
| | 0 °C | | 25 °C | | 40 °C | |
	Capacitance (F)	α	Capacitance (F)	α	Capacitance (F)	α
100 %	1369.3	0.486	672.9	0.474	11648.8	0.501
80%	174.1	0.477	200.5	0.465	12769.3	0.495
60%	153.2	0.489	210.2	0.502	14947.7	0.488
40%	131.4	0.460	186.9	0.512	14016.8	0.488
20%	139.2	0.453	166.3	0.482	7531.4	0.467
0%	253.4	0.511	129.4	0.471	3613.0	0.516

Fig. 8. Nyquist representations of temperature dependence of EIS at each SOC.
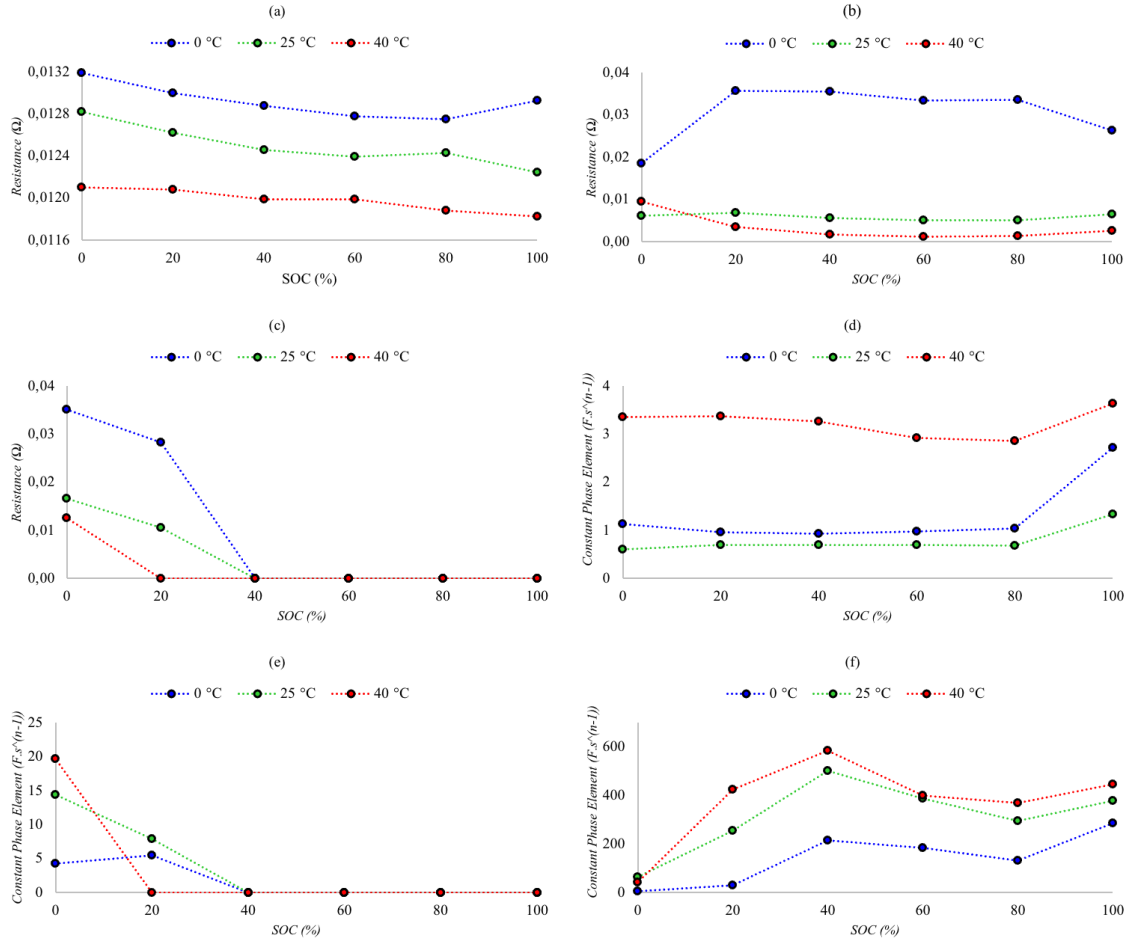
Fig. 9. Temperature dependence of (a) R_i, (b) R_{SEI}, (c) R_{CT}, (d) CPE_{SEI}, (e) CPE_{CT} and (f) CPE_{diff} vs. SOC.

4. CONCLUSION

The electrochemical performance of the batteries can be investigated by using both time-dependent and frequency-dependent measurements. To evaluate the electrical behaviour of the batteries from the measurement data, equivalent circuit modelling is considered. While 1 RC circuit model is used for pulse measurements to describe the DC charge transfer kinetics, for EIS measurements, 2 RC circuit model with constant phase element represents SEI resistance, charge transfer kinetics and diffusion behaviour. The temperature dependence of the electrochemical performance of the batteries is studied with various operating conditions. As described above, significant capacity loss and slow reaction kinetics were observed in low operating temperatures due to the graphite electrode's volume changes and SEI formation. The high-temperature performance of the batteries was slightly better due to the fast reaction kinetics. On the other hand, quick reactions and increased ambient temperature affect the cycle life of the batteries due to the cathode material limitations and vaporization of the electrolyte solution.

References

[1] J. M. Tarascon and M. Armand, "Issues and challenges facing rechargeable lithium batteries," *Nature*, 414(6861), pp. 359–367, 2001.

[2] J. Y. Yong, V. K. Ramachandaramurthy, K. M. Tan, and N. Mithulananthan, "A review on the state-of-the-art technologies of electric vehicle, its impacts and prospects," *Renew. Sustain. Energy Rev.*, vol. 49, pp. 365–385, September 2015.

[3] T. Waldmann, M. Wilka, M. Kasper, M. Fleischhammer, and M. Wohlfahrt-Mehrens, "Temperature dependent ageing mechanisms in Lithium-ion batteries – A Post-Mortem study," *J. Power Sources*, vol. 262, pp. 129–135, September 2014.

[4] T. C. Bach *et al.*, "Nonlinear ageing of cylindrical lithium-ion cells linked to heterogeneous compression," *J. Energy Storage*, vol. 5, pp. 212–223, January 2016.

[5] K. Jalkanen, J. Karppinen, L. Skogström, T. Laurila, M. Nisula, and K. Vuorilehto, "Cycle ageing of commercial NMC/graphite pouch cells at different temperatures," *Appl. Energy*, 154(C), pp. 160–172, 2015.

[6] Y. Du et al., "Capacity fade characteristics of nickel-based lithium-ion secondary battery after calendar deterioration at 80 °C," J. Power Sources, vol. 501, no. May, p. 230005, July 2021.

[7] L. Spitthoff, P. R. Shearing, and O. S. Burheim, "Temperature, ageing and thermal management of Lithium-Ion batteries," *Energies*, 14(5), p. 1248, 2021.

[8] J. C. Burns, D. A. Stevens, and J. R. Dahn, "In-Situ Detection of Lithium Plating Using High Precision Coulometry," *J. Electrochem. Soc.*, 162(6), pp. A959–A964, 2015.

[9] R. Hausbrand *et al.*, "Fundamental degradation mechanisms of layered oxide Li-ion battery cathode materials: Methodology, insights and novel approaches," *Mater. Sci. Eng. B*, vol. 192, pp. 3–25, February 2015.

[10] D. Ren *et al.*, "An electrochemical-thermal coupled overcharge-to-thermal-runaway model for lithium ion battery," *J. Power Sources*, vol. 364, pp. 328–340, October 2017.

[11] R. Guo, L. Lu, M. Ouyang, and X. Feng, "Mechanism of the entire overdischarge process and overdischarge-induced internal short circuit in lithium-ion batteries," *Sci. Rep.*, 6(1), p. 30248, 2016.

[12] Sony, "Lithium Ion Rechargeable Battery Technical Information," *Prog. Batter. Sol. Cells*, vol. 9, pp. 1–9, June 2012.

[13] A. Maheshwari, M. Heck, and M. Santarelli, "Cycle ageing studies of lithium nickel manganese cobalt oxide-based batteries using electrochemical impedance spectroscopy," *Electrochim. Acta*, vol. 273, pp. 335–348, May 2018.

[14] X. Han *et al.*, "A review on the key issues of the lithium ion battery degradation among the whole life cycle," *eTransportation*, vol. 1, p. 100005, August 2019.

[15] S. Lee and J. Kim, "Power capability analysis of lithium battery and supercapacitor by pulse duration," *Electron.*, 8(12), 2019.

[16] A. Rheinfeld *et al.*, "Quasi-Isothermal External Short Circuit Tests Applied to Lithium-Ion Cells: Part II. Modeling and Simulation," *J. Electrochem. Soc.*, 166(2), pp. A151–A177, 2019.

[17] M. Broussely *et al.*, "Main ageing mechanisms in Li-ion batteries," *J. Power Sources*, 146(1), pp. 90–96, 2005.

[18] G. J. Brug, A. L. G. van den Eeden, M. Sluyters-Rehbach, and J. H. Sluyters, "The analysis of electrode impedances complicated by the presence of a constant phase element," *J. Electroanal. Chem. Interfacial Electrochem.*, 176(1), pp. 275–295, 1984.

[19] J. R. Macdonald, "Impedance spectroscopy," *Ann. Biomed. Eng.*, 20(3), pp. 289–305, 1992.

Biographies

Ongun Bora Saban was born in Bartın, Turkey. After graduating from Bartın University Department of Mechanical Engineering, he started his master's degree in mechanical engineering at Gebze Technical University in 2018, where he works as a research assistant. He started his doctorate studies in 2020 in mechanical engineering at Gebze Technical University. His main research fields are Li-ion battery modelling, design optimization and electrochemical measurements.

E-mail: obsaban@gtu.edu.tr

Eda Güzel was born in Erzincan. She received the B.Sc. degree in electronics engineering from Gebze Technical University, Kocaeli, Turkey, in 2016, and the M.Sc. degree in electronics engineering from Gebze Technical University, Kocaeli, Turkey, in 2021. She completed her master's study on gPC Characterization of Filter AC Response. During her master's degree, she took part as a Project Engineer in the TÜBİTAK 1001 Research Support Program project titled "Development of a Battery Management System Based on Aging of Lithium-Ion Batteries".

E-mail: guzeleda@gmail.com

Mustafa Fazıl Serincan is Associate Prof. in Mechanical Engineering Department at Gebze Technical University. He holds a BSc (2003) degree in Mechanical Engineering from İstanbul Technical University. MSc (2005) degree in Electrical and Electronics Engineering and Computer Sciences from Sabancı University and PhD (2009) degree in mechanical engineering from University of Connecticut. His main research interests include Modeling of Li-ion batteries and fuel cells; Thermal management in aerospace applications, CFD solutions for transport phenomena from an engineering perspective.

E-mail: mfserincan@gtu.edu.tr

Mehmet Ali Arslan graduated from İstanbul Technical University Mechanical Engineering in 1989. After working as a research assistant at İstanbul Technical University Faculty of Mechanical Engineering in 1990-91, he went to the USA. He received his master's and Doctorate degrees from Rensselaer Polytechnic Institute, New York, in 1993 and 1998. He majored in Mechanical Engineering on Neural Networks/Intelligent Agents. He worked as Senior Engineer at Adapco Design & Analysis, NY Long Island until 2001 and Quest Global, Schenectady, NY until 2004. He studied many finite element analyses, mainly in aviation, energy, structure, etc. He has been working as a lecturer in the Department of Design and Manufacturing at Gebze Technical University since 2004. His main areas of study include structural finite element analysis, design optimization, composite materials analysis, experimental design and quality engineering.

E-mail: mehmet.arslan@gtu.edu.tr